BMJ Open Respiratory Research

High S100A9 level predicts poor survival, and the S100A9 inhibitor paquinimod is a candidate for treating idiopathic pulmonary fibrosis

Shinichiro Miura,[1] Hiroshi Iwamoto ,[1] Masashi Namba,[2] Kakuhiro Yamaguchi,[1] Shinjiro Sakamoto,[1] Yasushi Horimasu,[1] Takeshi Masuda,[1] Shintaro Miyamoto,[1] Taku Nakashima ,[1] Shinichiro Ohshimo,[3] Kazunori Fujitaka,[1] Hironobu Hamada,[4] Noboru Hattori[1]

To cite: Miura S, Iwamoto H, Namba M, *et al*. High S100A9 level predicts poor survival, and the S100A9 inhibitor paquinimod is a candidate for treating idiopathic pulmonary fibrosis. *BMJ Open Respir Res* 2024;**11**:e001803. doi:10.1136/bmjresp-2023-001803

► Additional supplemental material is published online only. To view, please visit the journal online (https://doi.org/10.1136/bmjresp-2023-001803).

Received 4 May 2023
Accepted 9 February 2024

For numbered affiliations see end of article.

Correspondence to
Dr Hiroshi Iwamoto; iwamotohiroshig@gmail.com

ABSTRACT

Background S100A9 is a damage-associated molecular pattern protein that may play an important role in the inflammatory response and fibrotic processes. Paquinimod is an immunomodulatory compound that prevents S100A9 activity. Its safety and pharmacokinetics have been confirmed in human clinical trials. In this study, we investigated the effects of paquinimod in preventing the development of lung fibrosis in vivo and examined the prognostic values of circulatory and lung S100A9 levels in patients with idiopathic pulmonary fibrosis (IPF).

Methods The expression and localisation of S100A9 and the preventive effect of S100A9 inhibition on fibrosis development were investigated in a mouse model of bleomycin-induced pulmonary fibrosis. In this retrospective cohort study, the S100A9 levels in the serum and bronchoalveolar lavage fluid (BALF) samples from 76 and 55 patients with IPF, respectively, were examined for associations with patient survival.

Results S100A9 expression was increased in the mouse lungs, especially in the inflammatory cells and fibrotic interstitium, after bleomycin administration. Treatment with paquinimod ameliorated fibrotic pathological changes and significantly reduced hydroxyproline content in the lung tissues of mice with bleomycin-induced pulmonary fibrosis. Additionally, we found that paquinimod reduced the number of lymphocytes and neutrophils in BALF and suppressed endothelial–mesenchymal transition in vivo. Kaplan-Meier curve analysis and univariate and multivariate Cox hazard proportion analyses revealed that high levels of S100A9 in the serum and BALF were significantly associated with poor prognoses in patients with IPF (Kaplan-Meier curve analysis: p=0.037 (serum) and 0.019 (BALF); multivariate Cox hazard proportion analysis: HR=3.88, 95% CI=1.06 to 14.21, p=0.041 (serum); HR=2.73, 95% CI=1.05 to 7.10, p=0.039 (BALF)).

Conclusions The present results indicate that increased S100A9 expression is associated with IPF progression and that the S100A9 inhibitor paquinimod is a potential treatment for IPF.

WHAT IS ALREADY KNOWN ON THIS TOPIC

⇒ S100A9 is a damage-associated molecular pattern protein that may play an important role in the inflammatory response and fibrotic processes.

⇒ Paquinimod is an immunomodulatory compound that prevents S100A9 activity, and it was well tolerated in human clinical trials.

WHAT THIS STUDY ADDS

⇒ Treatment with paquinimod prevented the development of lung fibrosis in a mouse model of bleomycin-induced pulmonary fibrosis.

⇒ Elevated S100A9 levels in the serum and bronchoalveolar lavage fluid were independent risk factors for poor prognosis in patients with idiopathic pulmonary fibrosis (IPF).

HOW THIS STUDY MIGHT AFFECT RESEARCH, PRACTICE OR POLICY

⇒ Circulatory and lung S100A9 are potential prognostic biomarkers in IPF, and the S100A9 inhibitor paquinimod is a potential new treatment for IPF.

INTRODUCTION

Idiopathic pulmonary fibrosis (IPF) is a progressive fibrotic lung disease with an unknown aetiology and a poor prognosis; it is characterised by irreversible destruction of the lung architecture.[1 2] The clinical course of IPF varies widely, from relatively stable to extremely rapidly progressive.[3] Recently, pirfenidone and nintedanib have been used for treating IPF, but their clinical effects are not entirely satisfactory owing to their limited efficacy and numerous side effects.[4–6] Therefore, there is a vital need for both effective biomarkers to predict the prognosis of patients and for a novel therapeutic option to halt disease progression and improve survival.

S100A9 (also known as myeloid-related protein 14 and calgranulin B) is an endogenous damage-associated molecular pattern protein that is mainly present in the cytoplasm of myeloid-derived cells, such as monocytes,

neutrophils and macrophages.[7 8] S100A9 is secreted in response to inflammatory conditions; it stimulates leucocyte recruitment and promotes secretion of inflammatory cytokines (such as interleukin (IL)-6, IL-1β and tumour necrosis factor-alpha (TNF-α)).[9–12] S100A9 is also associated with endothelial injury.[13 14] Increased expression of S100A9 has been confirmed in inflammatory diseases, such as systemic lupus erythematosus and systemic vasculitis.[12 15 16] Moreover, previous in vitro studies have shown that S100A9 promotes the proliferation of fibroblasts and increases the expression of collagen and α-smooth muscle actin (SMA)[17–19] and that inhibition of S100A9 activity ameliorates fibrosis in the liver and kidney in vivo.[20 21] In patients with IPF, S100A9 is highly expressed in the vascular endothelial cells and in areas of fibrotic remodelling in the lungs.[22] Additionally, S100A9 levels in the bronchoalveolar lavage fluid (BALF) are higher in patients with IPF than in healthy individuals and in patients with other interstitial lung diseases.[23 24] These reports suggest that S100A9 may be associated with the pathophysiology of IPF. However, the protective effects of S100A9 activity inhibition against lung fibrosis have not been clarified in vivo, and the prognostic values of circulatory and lung S100A9 levels in patients with IPF have not been elucidated.

In this study, we confirmed that S100A9 inhibition using the S100A9 inhibitor paquinimod prevented lung fibrosis development in a mouse model of bleomycin (BLM)-induced pulmonary fibrosis; the safety and pharmacokinetics of paquinimod have been confirmed in human clinical trials.[25 26] Additionally, we observed that paquinimod could reduce lung inflammation and endothelial–mesenchymal transition (EndMT) in vivo. Finally, we also found that elevated serum and BALF S100A9 levels were independent risk factors for poor prognosis in patients with IPF.

METHODS

Animals

Male C57BL/6 mice (6–8 weeks old) were purchased from Charles River Laboratories Japan (Yokohama, Japan). The mice were housed in pathogen-free rooms in a controlled environment under a 12-hour light–dark cycle. They were provided with free access to water and laboratory chow.

Development of mouse models of lung fibrosis and administration of the S100A9 inhibitor

The mice were randomly allocated into three groups: without BLM group (mice implanted with osmotic minipumps containing saline and intraperitoneally administered saline), BLM+saline group (mice implanted with osmotic minipumps containing BLM and intraperitoneally administered saline) and BLM+PQ group (mice implanted with osmotic minipumps containing BLM and intraperitoneally administered saline containing paquinimod).

On day 0, the mice were first anaesthetised with mixed anaesthetic agents, including medetomidine (0.3 mg/kg body weight; Kyoritsu Seiyaku, Tokyo, Japan), midazolam (4 mg/kg body weight; Sandoz K.K., Tokyo, Japan) and butorphanol (5 mg/kg body weight; Meiji Seika Pharma, Tokyo, Japan). The mice were then subcutaneously implanted with osmotic minipumps (Alzet Model 2001; Muromachi Kikai Co., Tokyo, Japan) containing saline or BLM (100 mg/kg body weight; Nippon Kayaku, Tokyo, Japan), as previously described.[27] They were then intraperitoneally administered saline or saline containing paquinimod (1.0 mg/kg body weight; Merck, Germany) daily until the end of the experiment. The osmotic minipumps were removed 10 days after implantation, as recommended by the manufacturer. The researchers were aware of the group allocation throughout the experiment. To minimise potential confounders arising from the animal or cage location, ventilated cages of each group were placed in the same room.

The mice were euthanized via exsanguination under anaesthesia. Briefly, the mice were first anaesthetised with mixed anaesthetic agents, namely medetomidine, midazolam and butorphanol. Thereafter, their aortas were cut for euthanasia via exsanguination.

Analysis of the BALF in mice

On days 14 and 28 after pump implantation, the BALF was obtained as previously described.[28] The total cell numbers were determined using an automated cell counter. Differential cell counts were obtained using the Diff-Quik stain (Kokusai Shiyaku, Kobe, Japan) and Cytospin (Thermo Fisher Scientific, Waltham, MA, USA).

Assessment of pulmonary fibrosis in mice

On day 28, after pump implantation, the lungs were harvested for a hydroxyproline assay and histological examination. The degree of pulmonary fibrosis was determined on the basis of the hydroxyproline content in the lung tissue, as previously described.[29] After perfusion with phosphate-buffered saline, the right lung was fixed with 4% paraformaldehyde and embedded in paraffin for histological examination. The sections were stained with H&E or azan.

Real-time qRT-PCR

Total cellular RNA was extracted from the lung tissues of mice using the RNeasy Mini Kit (Qiagen, Valencia, CA, USA) in accordance with the manufacturer's protocol. After extraction, the total RNA was converted into cDNA via reverse transcription, and real-time qRT-PCR was performed using an ABI 7500 Fast Real-Time PCR system (Applied Biosystems, Foster City, CA, USA). The mRNA expression levels were evaluated and normalised to those of β-actin as an endogenous reference. The following primers from Applied Biosystems were used: S100 calcium-binding protein A9 (S100A9), TaqMan

Gene Expression Assay ID Mm00656925_m1; E-cadherin, Mm01247357_m1; platelet and endothelial cell adhesion molecule 1 (PECAM1), Mm01242576_m1; cadherin 5, Mm00486938_m1; type I collagen α1 chain (COL1A1), Mm00801666_ g1; fibronectin, Mm01256744_m1 and β-actin, Mm02619580_g1.

Flow cytometry (FCM) analysis

Sample collection and FCM analyses were performed as previously described.[28] Briefly, single-cell suspensions were obtained as follows: the mice were euthanized (as described above), and their right lungs were excised, minced and digested in a Roswell Park Memorial Institute 1640 medium containing 1.0 mg/mL collagenase A (Roche Diagnostics, Basel, Switzerland) and 20 U/mL DNase I (Takara Bio, Shiga, Japan) at 37°C for 30 min. Red blood cells were lysed using the ammonium–chloride–potassium lysis buffer (Thermo Fisher Scientific). After blocking with antimouse CD16/32 Abs (FcγR, clone 93, BioLegend, San Diego, CA, USA), the cell suspensions were incubated with appropriate dilutions of antibodies or their isotype-matched controls. The rat monoclonal antibodies against mouse CD31 (MEC13.3), CD45 (30-F11) and CD326 (G8.8) were purchased from BioLegend. For intracellular staining, the cells were fixed and permeabilised using a Cytofix/Cytoperm Kit (BD Biosciences, San Jose, CA, USA); thereafter, they were stained with anti-α-SMA (mouse IgG2a, clone 1A4; Abcam). An isotype control antibody (mouse IgG2a, clone MOPC-173; BioLegend) was used to establish an α-SMA-positive gating region. $CD31^+$/CD45− cells and CD31−/CD45−/$CD326^+$ cells were defined as pulmonary vascular endothelial cells and epithelial cells, respectively.[30] α-SMA-positive vascular endothelial cells were defined as cells that underwent EndMT, whereas α-SMA-positive epithelial cells were defined as epithelial cells that underwent epithelial–mesenchymal transition (EMT).[31–33] The cells were analysed using BD FACS Aria II (BD Biosciences) or BD LSR Fortessa X-20 (BD Biosciences). The collected data were analysed using the FlowJo software (Tree Star, Ashland, OR, USA).

The methods of western blot analysis and immunohistochemical staining are described in online supplemental text file.

Patients with IPF

This was a retrospective cohort study on 86 patients who were newly diagnosed with IPF at the Hiroshima University Hospital between 2003 and 2015; their serum and BALF samples were obtained. The diagnosis of IPF was confirmed through a retrospective review based on international diagnostic criteria published in 2018.[34] Ten patients were excluded; these included those who experienced acute exacerbations of IPF within 1 month of diagnosis, those who were later diagnosed with fibrotic lung diseases other than IPF and those who underwent lung transplantation later.

Serum and BALF analyses and pulmonary function tests in patients with IPF

The serum and BALF samples were collected at diagnosis and stored at −80°C until the time of analysis. Bronchoalveolar lavage was performed as described previously.[35] Briefly, 50 mL of saline was promptly introduced into the lungs and subsequently suctioned and collected for further analyses; this procedure was repeated thrice. The BALF thus obtained was centrifuged promptly, and the supernatant was cryopreserved at −80°C until analysis. Serum samples were available for 76 patients with IPF (serum analysis group), whereas BALF samples were available for 55 patients with IPF (BALF analysis group). The S100A9 levels were measured using a commercially available ELISA kit in accordance with the manufacturer's instructions (CircuLex S100A9/MRP14 ELISA Kit; MBL International Corporation, Woburn, MA, USA). Pulmonary function variables were measured using spirometry (Chestac-55 V and Chestac-8800; CHEST, Tokyo, Japan) in accordance with the American Thoracic Society and European Respiratory Society recommendations.[36]

Statistical analyses

Data are expressed as mean±SEM unless indicated otherwise. Comparisons among groups were performed using the χ^2, Fisher's exact test and Mann–Whitney U test. The Spearman's rank correlation coefficient was used to determine the magnitude of the correlation between the percentage of α-SMA-positive endothelial cells measured from the right lung and the hydroxyproline content measured from the left lung of the same mouse. The Spearman's rank correlation coefficient was also calculated to reveal the association of the serum and BALF S100A9 levels with pulmonary function parameters and cell differentiation in the BALF of patients with IPF. We used receiver operating characteristic (ROC) curve analysis to determine the optimal serum and BALF S100A9 levels for predicting the 5-year survival rates in patients with IPF. The survival rate was calculated using the Kaplan-Meier approach and log-rank test. A Cox proportional hazards analysis was performed to identify the significant predictors of IPF prognosis. Age, sex, smoking status, forced vital capacity (FVC; % predicted), diffusing capacity for carbon monoxide (DLco; % predicted) and use of antifibrotic agents were included as independent variables in the multivariate analyses. Patients who were lost to follow-up were censored at the time of the last known contact. No criteria were set for animal exclusion a priori, and no experimental data points or animals were excluded from the analyses. Statistical significance was set at $p<0.05$. All data analyses were performed using JMP Pro V.15 (SAS Institute, Cary, NC, USA).

Patient and public involvement

The public and the patients were not involved in the designing, conducting, reporting and dissemination of this research.

Ethics approval and consent to participate

All experimental procedures of the experiments involving animals were approved by the Committee on Animal Research at Hiroshima University (approval no.: A18-28) and were conducted in accordance with the Guide for the Care and Use of Laboratory Animals (8th edition, 2010; National Institutes of Health, Bethesda, MD, USA). All procedures of experiments involving patients with IPF were approved by the Ethics Committee of the Hiroshima University Hospital (approval no.: M326) and were conducted in accordance with the ethical standards established in the Helsinki Declaration of 1975. All patients provided written informed consent.

RESULTS

Expression and localisation of S100A9 in the BLM-induced pulmonary fibrosis model

First, we investigated the expression and localisation of S100A9 in the lungs of mice subcutaneously treated with BLM. The S100A9 mRNA levels in the lung were upregulated, peaking on day 3 after implantation with osmotic minipumps containing BLM (online supplemental figure S1A). The S100A9 protein-expression levels were also increased, peaking on days 3–7 after BLM treatment; this increased expression continued until day 21 (online supplemental figure S1B). Immunohistochemical staining revealed a high expression of S100A9 in the inflammatory cells in both the central and subpleural regions of the lung as well as in the fibrotic interstitium, especially on day 14 (online supplemental figure S1C).

S100A9 inhibitor paquinimod ameliorates BLM-induced pulmonary fibrosis

We then investigated whether paquinimod prevented lung fibrosis development in a mouse model of BLM-induced pulmonary fibrosis. The experimental scheme is illustrated in figure 1A. Paquinimod administration significantly suppressed the number of lymphocytes in the BALF at 14 and 28 days after BLM treatment and suppressed the number of neutrophils at 28 days after BLM treatment (figure 1B). As shown in figure 1C, the increase in the hydroxyproline content in the lungs in response to BLM was significantly reduced by paquinimod administration. Histological analyses revealed that paquinimod administration reduced the extent of fibrotic changes and the degree of collagen deposition in BLM-injured mice (figure 1D). The increased S100A9 expression in the lungs in response to BLM was not altered by

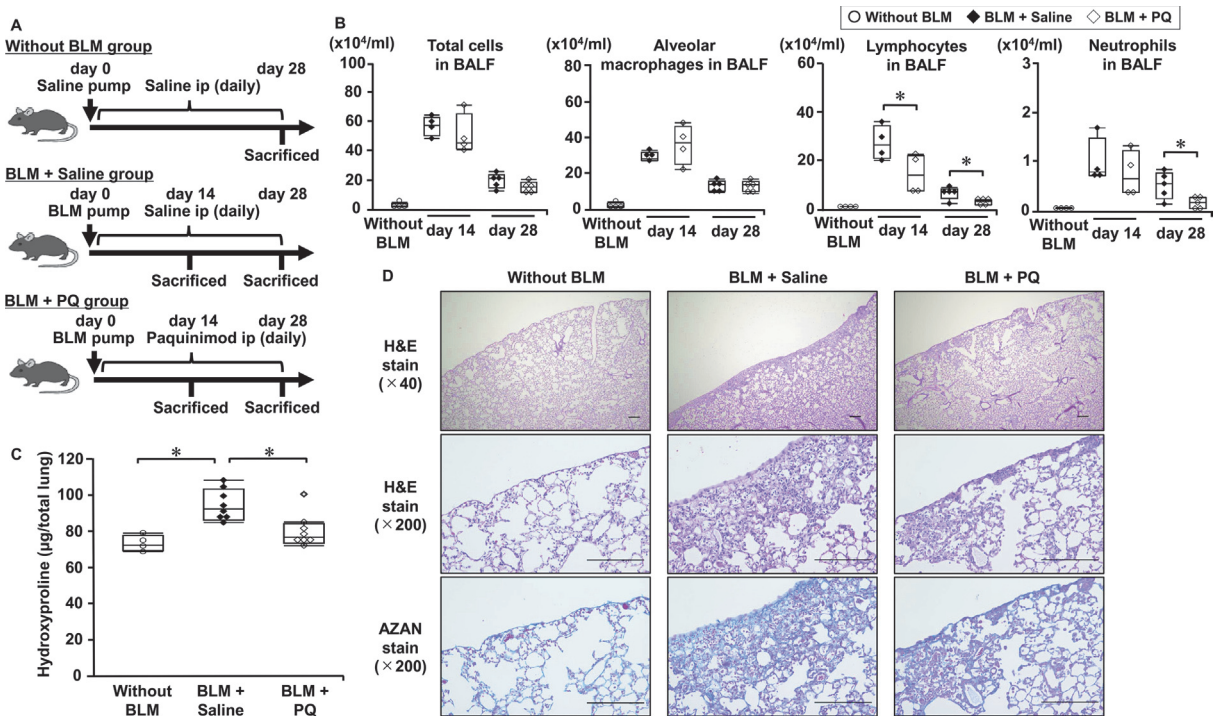

Figure 1 Effect of PQ on BLM-induced pulmonary fibrosis in mice. (A) Experimental scheme. The mice were allocated into three groups: without BLM group (mice implanted with osmotic minipumps containing saline and intraperitoneally administered saline), BLM+saline group (mice implanted with osmotic minipumps containing BLM and intraperitoneally administered saline) and BLM+PQ group (mice implanted with osmotic minipumps containing BLM and intraperitoneally administered saline containing the S100A9 inhibitor paquinimod). (B) Inflammatory cells in the bronchoalveolar lavage fluid at 14 or 28 days after BLM administration (n=4–5 per group). (C) The hydroxyproline content in the whole lungs at 28 days after BLM administration (n=4–8 per group). (D) Histological analysis of the lung at 28 days after BLM administration. Scale bar=200 μm. Data are presented as box-and-whisker plots; boxes represent the 25th to 75th percentiles, solid lines within the boxes show the median values, and whiskers represent the 10th and 90th percentiles. *p<0.05. BLM, bleomycin; PQ, paquinimod.

paquinimod administration (online supplemental figure S2).

EndMT is involved in the fibrotic process in a mouse model of subcutaneous BLM-induced pulmonary fibrosis

Previous in vitro studies have demonstrated that S100A9 decreases the expression of endothelial cell junction proteins and induces endothelial monolayer hyperpermeability.[13 14] Based on these observations, we hypothesised that S100A9 may be involved in the pathogenesis of IPF by altering the characteristics of endothelial cells and inducing EndMT (a process wherein the endothelial cells lose their endothelial cell phenotype and acquire a mesenchymal cell phenotype).[37]

Before testing the above-mentioned hypothesis, we first assessed the gene expression of endothelial, epithelial and mesenchymal markers and evaluated cell populations, especially focusing on EndMT and EMT in the subcutaneous BLM-induced mouse model of pulmonary fibrosis. Decreased gene expression of epithelial markers (E-cadherin) and endothelial markers (Pecam1 and Cadherin5) and increased gene expression of mesenchymal markers (Col1a1 and Fibronectin) were observed in mouse lungs at 14–28 days after BLM administration (online supplemental figure S3A). The experimental scheme of the FCM analysis is shown in online supplemental figure S3B. FCM analyses demonstrated that compared with non-treated mouse lungs, the percentage of α-SMA-positive cells was significantly increased in the endothelial cells, and the percentage of endothelial cells in the lung constituent cells (CD45– cells) was significantly decreased at 28 days in BLM-treated mouse lungs (online supplemental figure S3C). These results indicated that EndMT is involved in the fibrotic process in mice with pulmonary fibrosis induced by subcutaneously administered BLM. The percentages of total epithelial cells and of α-SMA-positive epithelial cells did not change significantly after BLM administration.

Paquinimod suppressed EndMT in the mouse model with BLM-induced pulmonary fibrosis

Paquinimod administration attenuated BLM-induced changes in the gene expression of endothelial and mesenchymal markers in the lungs at 14 days after BLM administration (figure 2A). Thus, we hypothesised that paquinimod may reduce EndMT, and the FCM analysis was performed to test this hypothesis. The percentage of α-SMA-positive endothelial cells decreased and that of

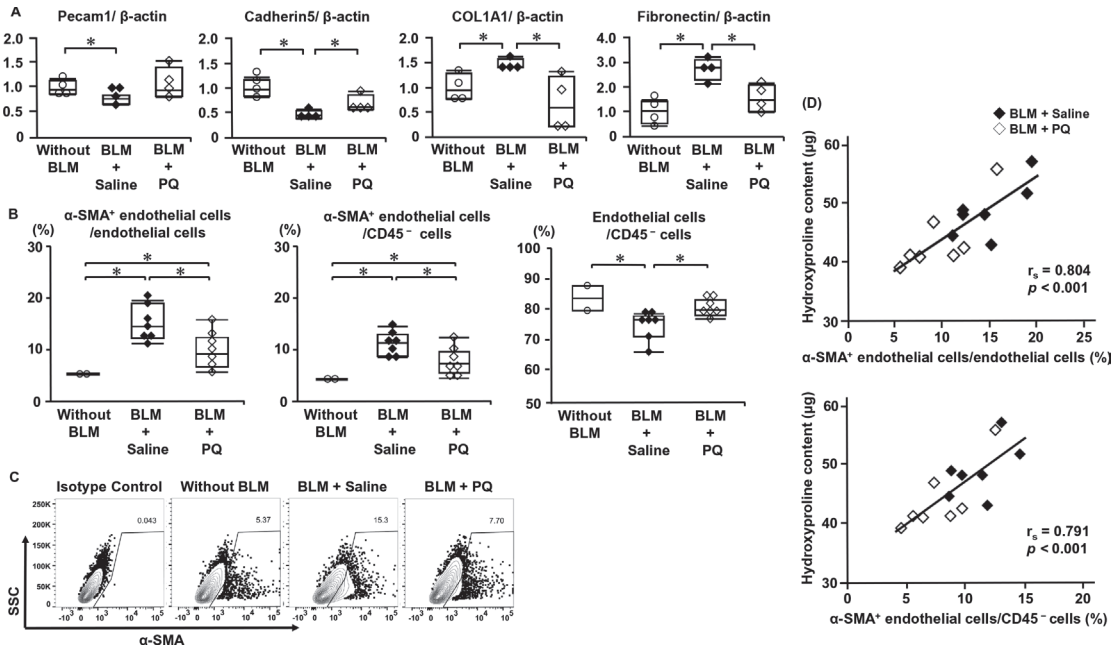

Figure 2 Association between the preventive effects of PQ against fibrosis development and EndMT inhibition in BLM-induced pulmonary fibrosis in mice. The expression of markers associated with EndMT was evaluated in the lungs of mice without BLM, BLM+saline and BLM+PQ groups. (A) Gene expression of endothelial-specific markers (Pecam1 and Cadherin5) and mesenchymal-specific markers (COL1A1 and Fibronectin) was evaluated using real-time quantitative reverse-transcription PCR 14 days after BLM administration (n=4 per group). (B) The percentage of α-SMA-positive endothelial cells in the total endothelial cells and lung constituent cells (CD45– cells) and the percentage of total endothelial cells in the CD45– cells were evaluated using flow cytometry analyses at 28 days after BLM administration (n=2–7 per group). (C) Representative flow cytometry panels showing α-SMA expression in endothelial cells. (D) The correlation between the percentages of α-SMA-positive endothelial cells and the hydroxyproline content in the BLM+saline and BLM+PQ groups at 28 days after BLM administration (n=7 per group). Data are presented as box-and-whisker plots; boxes represent the 25th to 75th percentiles, solid lines within the boxes show the median values, and whiskers represent the 10th and 90th percentiles. *p<0.05. BLM, bleomycin; EndMT, endothelial–mesenchymal transition; PQ, paquinimod.

Table 1 Baseline characteristics of patients with IPF

Variables	Patients with IPF	
	Serum	BALF
Patients, n	76	55
Age, years	67.9±8.7	66.7±8.6
Sex, male/female	67/9	51/4
Body mass index, kg/m²	24.4±3.2	24.5±3.2
Smoking status, n (%)		
Never smoker	11 (14.5)	6 (10.9)
Ever smoker with <10 pack-years	6 (7.9)	4 (7.3)
Ever smoker with ≥10 pack-years	59 (77.6)	45 (81.8)
Pulmonary function parameters		
Forced vital capacity, % predicted	76.9±18.5	77.5±19.3
Diffusing capacity for carbon monoxide, % predicted	50.1±14.9	51.1±15.2
BALF analysis		
Total cell count, $\times 10^4$/mL	–	21.1±15.3
Macrophage, %	–	83.5±9.9
Lymphocyte, %	–	11.4±9.9
Neutrophil, %	–	3.4±3.3
Eosinophil, %	–	1.6±1.6
S100A9 concentration, ng/mL	12.3±12.5	7.6±10.5

Variables are presented as mean±SD unless stated otherwise.
BALF, bronchoalveolar lavage fluid; IPF, idiopathic pulmonary fibrosis.

total endothelial cells in the lungs increased following paquinimod treatment at 28 days after BLM administration (figure 2B,C). Moreover, we observed positive correlations between the percentage of α-SMA-positive endothelial cells and hydroxyproline content in the BLM+saline and BLM+PQ groups (figure 2D).

Baseline characteristics and the serum and BALF S100A9 levels in patients with IPF

The baseline characteristics of the patients with IPF are presented in table 1. The mean age was approximately 65 years, and more than 80% of the patients were men and smokers in both the serum and BALF analysis groups. The mean FVC and DLco (% predicted) were approximately 75% and 50%, respectively, in both the serum and BALF analysis groups. The mean serum and BALF S100A9 concentrations were 12.3±12.5 ng/mL and 7.6±10.5 ng/mL, respectively. The BALF S100A9 levels were positively correlated with the neutrophil number and percentage in the BALF (online supplemental table S1).

Prognostic value of S100A9 levels in patients with IPF

The median observation period was 52.5 months. ROC curve analysis revealed that the optimal cut-off levels of S100A9 for predicting the 5-year survival rates were 7.30 ng/mL in the serum analysis group and 6.44 ng/mL in the BALF analysis group, as determined by the area under the curve values of 0.59 and 0.61, respectively (online supplemental figure S4). The Kaplan-Meier method and the log-rank test showed that the survival rates were significantly lower in patients with higher S100A9 levels in both the serum and BALF analysis groups (p=0.037 and p=0.019, respectively; figure 3). Univariate and multivariate Cox proportional hazard analyses showed that higher S100A9 levels in both the serum and BALF were independently associated with poorer prognoses in patients with IPF (table 2).

DISCUSSION

Using a mouse model of BLM-induced pulmonary fibrosis, we showed that the S100A9 expression increased in mouse lungs after BLM administration and that treatment with the S100A9 inhibitor paquinimod prevented lung fibrosis development in this model. This study also demonstrated that higher serum and BALF S100A9 levels were risk factors for poorer prognoses in patients with IPF. These results indicate that an increased S100A9 expression may play an important role in the pathophysiology of IPF and could be a treatment target. Additionally, we showed that paquinimod could reduce lung inflammation and EndMT in this model, again supporting a

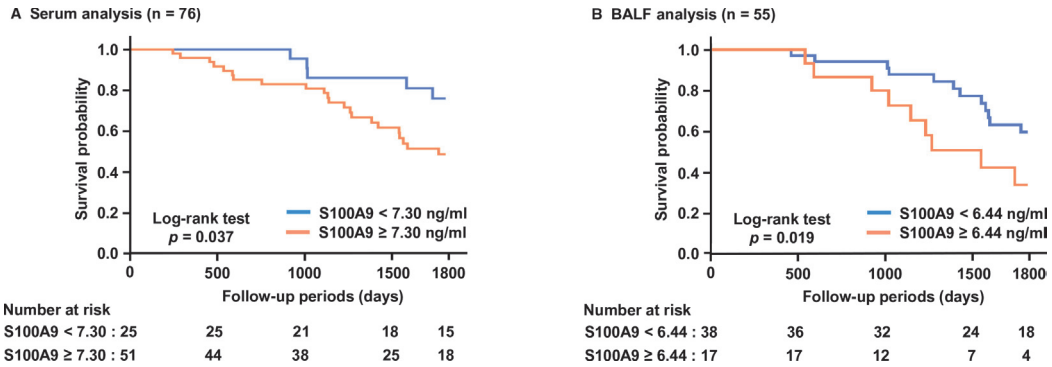

Figure 3 Five-year survival in patients with IPF based on the S100A9 levels in the serum and BALF. High S100A9 levels in both the (A) serum and (B) BALF were significantly associated with poor survival in patients with IPF. BALF, bronchoalveolar lavage fluid; IPF, idiopathic pulmonary fibrosis.

Table 2 Predictive value for the 5-year mortality in patients with IPF, as assessed using a Cox proportional hazard model

	Univariate analysis			Multivariate analysis		
Variables	HR	95% CI	P value	HR	95% CI	P value
Serum (n=76)						
Age, years	0.99	0.96 to 1.04	0.985	–	–	–
Male (vs female)	2.97	0.40 to 21.94	0.285	–	–	–
Ever smoking with ≥10 pack-years (vs never or smoking with <10 pack-years)	1.33	0.40 to 4.42	0.646	–	–	–
FVC, % predicted	0.95	0.92 to 0.98	<0.001*	0.95	0.92 to 0.98	0.005*
DLco, % predicted	0.96	0.93 to 0.99	0.021*	0.98	0.94 to 1.02	0.256
Use of antifibrotic agent	1.49	0.69 to 3.22	0.307	–	–	–
Serum S100A9, ≥7.30 ng/mL	2.71	1.02 to 7.17	0.045*	3.88	1.06 to 14.21	0.041*
BALF (n=55)						
Age, years	1.01	0.96 to 1.06	0.706	–	–	–
Male (vs female)	1.00	0.13 to 7.51	0.996	–	–	–
Ever smoking with 10 pack-years (vs never or smoking with <10 pack-years)	0.51	0.15 to 1.75	0.286	–	–	–
FVC, % predicted	0.97	0.94 to 0.99	0.010*	0.97	0.95 to 1.00	0.095
DLco, % predicted	0.95	0.92 to 0.99	0.011*	0.95	0.91 to 0.99	0.031*
Use of antifibrotic agent	1.36	0.58 to 3.18	0.482	–	–	–
BALF S100A9, ≥6.44 ng/mL	2.64	1.13 to 6.15	0.024*	2.73	1.05 to 7.10	0.039*

*p<0.05, Cox proportional hazards model.
BALF, bronchoalveolar lavage fluid; DLco, diffusing capacity for carbon monoxide; FVC, forced vital capacity; IPF, idiopathic pulmonary fibrosis.

possible mechanism of S100A9 in the pathophysiology of lung fibrosis.

The present study showed that higher serum and BALF S100A9 levels were independently associated with poorer prognoses in patients with IPF. Previous studies have shown that an elevated BALF S100A9 level is a characteristic feature of IPF and is associated with reduced lung function in patients with IPF.[23 24 38 39] Additionally, a recent study showed that increased serum S100A9 levels were associated with poorer short-term survival (3 months) after acute exacerbation of IPF.[38] Our clinical data further support that an increased S100A9 expression is associated with IPF progression. Moreover, we demonstrated that S100A9 inhibition using paquinimod prevented lung fibrosis development in a preclinical model of IPF. Paquinimod is a small-molecule inhibitor that blocks the binding of S100A9 to toll-like receptor 4 and the receptor for advanced glycation end products.[40] Importantly, paquinimod was reported to have fewer side effects and encouraging pharmacokinetics in early phase trials on patients with systemic lupus erythematosus and systemic sclerosis.[25 26] Taken together, our results indicate that circulatory and lung S100A9 are potential prognostic biomarkers and that the S100A9 inhibitor paquinimod is a potential new treatment for IPF.

The present study showed that administering an S100A9 inhibitor reduced the BALF neutrophil count in a BLM-induced pulmonary fibrosis model. Additionally, a significant positive correlation was observed between the BALF S100A9 levels and the number of BALF neutrophils in patients with IPF; this is in agreement with previous reports.[22 23] Previous studies have shown that S100A9 induces neutrophil infiltration into tissues[41 42]; furthermore, Kinder *et al* reported that BALF neutrophilia predicts early mortality in IPF.[43] Neutrophils secrete various mediators, such as neutrophil elastase, TNF-α, matrix metalloproteinases, reactive oxygen and neutrophil extracellular traps, which are involved in epithelial cell damage, extracellular matrix degradation and synthesis, fibroblast activation and induction of EndMT.[44–46] These reports suggest that neutrophil-mediated injury facilitated by S100A9 plays an important role in epithelial damage and fibrosis. Moreover, the results of the present study also indicated that paquinimod could reduce EndMT in the mouse model of BLM-induced pulmonary fibrosis. A reduced expression of endothelial markers and an increased expression of mesenchymal markers were observed in this model, and administration of paquinimod attenuated the altered gene expression of these markers. Additionally, paquinimod reduced the number of α-SMA-positive endothelial cells, which was in parallel with the reduction of the hydroxyproline content in the BLM-induced lung fibrosis mouse model. Taken together, these results suggest that S100A9 inhibition protects against lung fibrosis via the inhibition of lung inflammation and EndMT; however,

further in vitro studies are warranted to elucidate the underlying mechanisms.

In the present study, S100A9 expression in the lungs was not suppressed by paquinimod administration at either the gene or the protein level in vivo. Although several studies have revealed the therapeutic effects of paquinimod, such as suppression of neutrophil infiltration into tissues and suppression of inflammatory cytokine production,[20 47 48] it is unclear whether paquinimod alters the expression of S100A9. Generally, inhibitors do not necessarily suppress the expression of their target molecules. TNF inhibitors, such as infliximab and etanercept, and IL-6 inhibitors, such as tocilizumab, which inhibit the activity of secreted TNF-α and IL-6 respectively, do not reduce the levels of these cytokines in the blood.[49–51] The prolonged half-life or impeded clearance of the inhibited substances may explain this phenomenon. Paquinimod works by binding to secreted S100A9 and inhibiting its binding to receptors.[40 52] Therefore, paquinimod may inhibit the effects of S100A9 without suppressing its expression. Further studies are necessary to validate this.

Myofibroblasts are the cells responsible for the establishment and progression of the fibrotic process.[53–55] They can originate from various sources, such as from quiescent tissue fibroblasts and from the phenotypic transition of various cell types into activated myofibroblasts (a process called EMT and EndMT for epithelial and endothelial cells, respectively).[37 56 57] Previous studies have shown that S100A9 promotes the proliferation and activation of fibroblasts[17–19] and induces EMT.[58] The present study has shown the possibility that S100A9 is associated with EndMT and neutrophil accumulation in the lungs. Taken together, S100A9 may be involved in the disease progression and pathogenesis of IPF through various mechanisms, such as by inducing fibroblast proliferation and activation, EMT, EndMT and neutrophil infiltration into the lungs; all of these result in the destruction of alveolar structures and abnormal tissue repair.

This study has several limitations. First, although this study demonstrated an association of S100A9 with EndMT in vivo, the detailed mechanisms underlying this association were not elucidated and require further studies. Second, paquinimod administration was initiated immediately after BLM injection, because the S100A9 protein-expression levels increased, peaking on days 3–7 after BLM injection. To assess the antifibrotic effect of paquinimod, it may have been better to initiate paquinimod administration on day 14 after BLM injection instead, that is, when the fibrotic phase of subcutaneous BLM-induced pulmonary fibrosis is generally considered to begin.[27 59 60] However, the limitations of an animal model made it difficult to determine the appropriate duration of drug administration for the accurate assessment of the antifibrotic effect. The BLM model is an approximation of the presentation of severe IPF and does not recapitulate the aetiology of clinical disease. Third, the clinical data of patients with IPF from only a single institution were examined; therefore, the sample size was relatively small. Additionally, a power analysis was not performed because of the study's retrospective design. Fourth, the presence of a gender bias could not be ruled out in this study. A higher prevalence in men as compared with women has been reported as a clinical feature of IPF, especially in the Japanese population.[61–64] Consistent with these previous reports, over 80% of the study participants were men, and male animals were used in this study accordingly. Although the patients from both sexes did not differ significantly in terms of the S100A9 levels and the baseline characteristics (except for the smoking history; online supplemental table S2), the number of the included women was too small. Furthermore, the present study did not investigate the therapeutic effects of paquinimod in female mice. All of these factors could have led to a gender bias.

CONCLUSIONS

This study revealed that higher serum and BALF S100A9 levels were independently associated with poorer prognoses in patients with IPF and that S100A9 inhibition prevented lung fibrosis development in a BLM-induced pulmonary fibrosis mouse model. The present results indicate that an increased expression of S100A9 is associated with the progression of IPF and that the S100A9 inhibitor paquinimod has the potential to treat IPF.

Author affiliations
[1]Department of Molecular and Internal Medicine, Graduate School of Biomedical and Health Sciences, Hiroshima University, Hiroshima, Japan
[2]Department of Clinical Oncology, Graduate School of Biomedical and Health Sciences, Hiroshima University, Hiroshima, Japan
[3]Department of Emergency and Critical Care Medicine, Graduate School of Biomedical and Health Sciences, Hiroshima University, Hiroshima, Japan
[4]Department of Physical Analysis and Therapeutic Sciences, Graduate School of Biomedical and Health Sciences, Hiroshima University, Hiroshima, Japan

Acknowledgements We thank Ms Yukari Iyanaga (Department of Molecular and Internal Medicine, Graduate School of Biomedical and Health Sciences, Hiroshima University) and Ms Yoko Hayashi (Natural Science Center for Basic Research and Development, Hiroshima University) for their excellent technical assistance. We thank Editage (www.editage.com) for English language editing. Part of this work was carried out at the Research Facilities for Laboratory Animal Science, Hiroshima University. This study was supported by the Program of the Network-Type Joint Usage/Research Center for Radiation Disaster Medical Science.

Contributors S.Miura contributed to data collection, data analysis, interpretation and manuscript writing. HI contributed to the conception and design, data collection, financial support, data analysis, interpretation and manuscript writing. HI is the guarantor. KY, YH, S.Miyamoto, TN, SO and HH contributed to data analysis and interpretation, reviewed the manuscript for important intellectual content and approved its submission. MN, SS, TM and KF contributed to the review of the manuscript for important intellectual content and approval for submission. NH contributed to the conception and design, financial support, review of the manuscript for important intellectual content and approval for submission. All the authors have read and approved the manuscript.

Funding This work was supported by a Grant-in-Aid for scientific research from the Ministry of Education, Culture, Sports, Science and Technology of Japan (17K09655).

Competing interests None declared.

Patient and public involvement Patients and/or the public were not involved in the design, or conduct, or reporting, or dissemination plans of this research.

Patient consent for publication Not applicable.

Ethics approval This study involves human participants. All procedures of experiments involving patients with IPF were approved by the Ethics Committee

of the Hiroshima University Hospital (approval no.: M326) and were conducted in accordance with the ethical standards established in the Helsinki Declaration of 1975. Participants gave informed consent to participate in the study before taking part.

Provenance and peer review Not commissioned; externally peer reviewed.

Data availability statement Data are available upon reasonable request.

ORCID iDs
Hiroshi Iwamoto http://orcid.org/0000-0003-4922-5334
Taku Nakashima http://orcid.org/0000-0002-0035-674X

REFERENCES

1 King TE, Pardo A, Selman M. Idiopathic pulmonary fibrosis. *Lancet* 2011;378:1949–61.
2 Raghu G, Collard HR, Egan JJ, *et al*. An official ATS/ERS/JRS/ALAT statement: idiopathic pulmonary fibrosis: evidence-based guidelines for diagnosis and management. *Am J Respir Crit Care Med* 2011;183:788–824.
3 Ley B, Collard HR, King TE. Clinical course and prediction of survival in idiopathic pulmonary fibrosis. *Am J Respir Crit Care Med* 2011;183:431–40.
4 Barratt SL, Creamer A, Hayton C, *et al*. Idiopathic pulmonary fibrosis (IPF): an overview. *J Clin Med* 2018;7:201.
5 Nathan SD, Costabel U, Glaspole I, *et al*. Efficacy of Pirfenidone in the context of multiple disease progression events in patients with idiopathic pulmonary fibrosis. *Chest* 2019;155:712–9.
6 Albera C, Costabel U, Fagan EA, *et al*. Efficacy of Pirfenidone in patients with idiopathic pulmonary fibrosis with more preserved lung function. *Eur Respir J* 2016;48:843–51.
7 Vogl T, Ludwig S, Goebeler M, *et al*. MRP8 and MRP14 control Microtubule reorganization during transendothelial migration of phagocytes. *Blood* 2004;104:4260–8.
8 Foell D, Wittkowski H, Vogl T, *et al*. S100 proteins expressed in phagocytes: a novel group of damage-associated molecular pattern molecules. *J Leukoc Biol* 2007;81:28–37.
9 Simard JC, Girard D, Tessier PA. Induction of neutrophil degranulation by S100A9 via a MAPK-dependent mechanism. *J Leukoc Biol* 2010;87:905–14.
10 Ehrchen JM, Sunderkötter C, Foell D, *et al*. The endogenous toll-like receptor 4 agonist S100A8/S100A9 (Calprotectin) as innate amplifier of infection, autoimmunity, and cancer. *J Leukoc Biol* 2009;86:557–66.
11 Anceriz N, Vandal K, Tessier PA. S100A9 mediates neutrophil adhesion to fibronectin through activation of Beta2 integrins. *Biochem Biophys Res Commun* 2007;354:84–9.
12 Wang S, Song R, Wang Z, *et al*. S100A8/A9 in inflammation. *Front Immunol* 2018;9:1298.
13 Viemann D, Strey A, Janning A, *et al*. Myeloid-related proteins 8 and 14 induce a specific inflammatory response in human microvascular endothelial cells. *Blood* 2005;105:2955–62.
14 Wang L, Luo H, Chen X, *et al*. Functional characterization of S100A8 and S100A9 in altering monolayer permeability of human umbilical endothelial cells. *PLoS ONE* 2014;9:e90472.
15 Soyfoo MS, Roth J, Vogl T, *et al*. Phagocyte-specific S100A8/A9 protein levels during disease exacerbations and infections in systemic lupus erythematosus. *J Rheumatol* 2009;36:2190–4.
16 Bai X, Xu P-C, Chen T, *et al*. The potential pathogenic roles of S100A8/A9 and S100A12 in patients with MPO-ANCA-positive vasculitis. *BMC Immunol* 2022;23:42.
17 Shibata F, Miyama K, Shinoda F, *et al*. Fibroblast growth-stimulating activity of S100A9 (MRP-14). *Eur J Biochem* 2004;271:2137–43.
18 Xu X, Chen H, Zhu X, *et al*. S100A9 promotes human lung fibroblast cells activation through receptor for advanced glycation end-product-mediated extracellular-regulated kinase 1/2, mitogen-activated protein-kinase and nuclear factor-kappaB-dependent pathways. *Clin Exp Immunol* 2013;173:523–35.
19 Araki K, Kinoshita R, Tomonobu N, *et al*. The heterodimer S100A8/A9 is a potent therapeutic target for idiopathic pulmonary fibrosis. *J Mol Med (Berl)* 2021;99:131–45.
20 Fransén Pettersson N, Deronic A, Nilsson J, *et al*. The immunomodulatory quinoline-3-carboxamide paquinimod reverses established fibrosis in a novel mouse model for liver fibrosis. *PLoS One* 2018;13:e0203228.
21 Tammaro A, Florquin S, Brok M, *et al*. S100A8/A9 promotes parenchymal damage and renal fibrosis in obstructive nephropathy. *Clin Exp Immunol* 2018;193:361–75.
22 Bargagli E, Olivieri C, Cintorino M, *et al*. Calgranulin B (S100A9/Mrp14): a key molecule in idiopathic pulmonary fibrosis. *Inflammation* 2011;34:85–91.
23 Hara A, Sakamoto N, Ishimatsu Y, *et al*. S100A9 in BALF is a candidate biomarker of idiopathic pulmonary fibrosis. *Respir Med* 2012;106:571–80.
24 Bargagli E, Olivieri C, Prasse A, *et al*. Calgranulin B (S100A9) levels in Bronchoalveolar lavage fluid of patients with interstitial lung diseases. *Inflammation* 2008;31:351–4.
25 Bengtsson AA, Sturfelt G, Lood C, *et al*. Pharmacokinetics, tolerability, and preliminary efficacy of paquinimod (ABR-215757), a new Quinoline-3-carboxamide derivative: studies in lupus-prone mice and a multicenter, randomized, double-blind, placebo-controlled, repeat-dose, dose-ranging study in patients with systemic lupus erythematosus. *Arthritis Rheum* 2012;64:1579–88.
26 Hesselstrand R, Distler JHW, Riemekasten G, *et al*. An open-label study to evaluate biomarkers and safety in systemic sclerosis patients treated with Paquinimod. *Arthritis Res Ther* 2021;23:204.
27 Aono Y, Nishioka Y, Inayama M, *et al*. Imatinib as a novel antifibrotic agent in bleomycin-induced pulmonary fibrosis in mice. *Am J Respir Crit Care Med* 2005;171:1279–85.
28 Takao S, Nakashima T, Masuda T, *et al*. Human bone marrow-derived mesenchymal stromal cells cultured in serum-free media demonstrate enhanced antifibrotic abilities via prolonged survival and robust regulatory T cell induction in murine bleomycin-induced pulmonary fibrosis. *Stem Cell Res Ther* 2021;12:506.
29 Hattori N, Degen JL, Sisson TH, *et al*. Bleomycin-induced pulmonary fibrosis in fibrinogen-null mice. *J Clin Invest* 2000;106:1341–50.
30 Tsukui T, Ueha S, Abe J, *et al*. Qualitative rather than quantitative changes are hallmarks of fibroblasts in bleomycin-induced pulmonary fibrosis. *Am J Pathol* 2013;183:758–73.
31 Suzuki T, Tada Y, Nishimura R, *et al*. Endothelial-to-mesenchymal transition in lipopolysaccharide-induced acute lung injury drives a progenitor cell-like phenotype. *Am J Physiol Lung Cell Mol Physiol* 2016;310:L1185–98.
32 Suzuki T, Tada Y, Gladson S, *et al*. Vildagliptin ameliorates pulmonary fibrosis in lipopolysaccharide-induced lung injury by inhibiting endothelial-to-Mesenchymal transition. *Respir Res* 2017;18:177.
33 Du S-F, Wang X-L, Ye C-L, *et al*. Exercise training ameliorates bleomycin-induced epithelial mesenchymal transition and lung fibrosis through restoration of H(2) S synthesis. *Acta Physiol (Oxf)* 2019;225:e13177.
34 Raghu G, Remy-Jardin M, Myers J, *et al*. The 2018 diagnosis of idiopathic pulmonary fibrosis guidelines: surgical lung biopsy for radiological pattern of probable usual interstitial pneumonia is not mandatory. *Am J Respir Crit Care Med* 2019;200:1089–92.
35 Yamaguchi K, Iwamoto H, Mazur W, *et al*. Reduced endogenous secretory RAGE in blood and bronchoalveolar Lavage fluid is associated with poor prognosis in idiopathic pulmonary fibrosis. *Respir Res* 2020;21:145.
36 Miller MR, Crapo R, Hankinson J, *et al*. General considerations for lung function testing. *Eur Respir J* 2005;26:153–61.
37 Piera-Velazquez S, Mendoza FA, Jimenez SA. Endothelial to mesenchymal transition (EndoMT) in the pathogenesis of human Fibrotic diseases. *J Clin Med* 2016;5:45.
38 Machahua C, Guler SA, Horn MP, *et al*. Serum calprotectin as new biomarker for disease severity in idiopathic pulmonary fibrosis: a cross-sectional study in two independent cohorts. *BMJ Open Respir Res* 2021;8:e000827.
39 Bennett D, Salvini M, Fui A, *et al*. Calgranulin B and KL-6 in Bronchoalveolar Lavage of patients with IPF and NSIP. *Inflammation* 2019;42:463–70.
40 Björk P, Björk A, Vogl T, *et al*. Identification of human S100A9 as a novel target for treatment of autoimmune disease via binding to Quinoline-3-Carboxamides. *PLoS Biol* 2009;7:e1000097.

41 Chen B, Miller AL, Rebelatto M, *et al*. S100A9 induced inflammatory responses are mediated by distinct damage associated molecular patterns (DAMP) receptors in vitro and in vivo. *PLoS ONE* 2015;10:e0115828.
42 Ryckman C, Vandal K, Rouleau P, *et al*. Proinflammatory activities of S100: proteins S100A8, S100A9, and S100A8/A9 induce neutrophil Chemotaxis and adhesion. *J Immunol* 2003;170:3233–42.
43 Kinder BW, Brown KK, Schwarz MI, *et al*. Baseline BAL neutrophilia predicts early mortality in idiopathic pulmonary fibrosis. *Chest* 2008;133:226–32.
44 Grommes J, Soehnlein O. Contribution of neutrophils to acute lung injury. *Mol Med* 2011;17:293–307.
45 Ishikawa G, Liu A, Herzog EL. Evolving perspectives on innate immune mechanisms of IPF. *Front Mol Biosci* 2021;8:676569.
46 Pieterse E, Rother N, Garsen M, *et al*. Neutrophil extracellular traps drive endothelial-to-mesenchymal transition. *Arterioscler Thromb Vasc Biol* 2017;37:1371–9.
47 Railwah C, Lora A, Zahid K, *et al*. Cigarette smoke induction of S100A9 contributes to chronic obstructive pulmonary disease. *Am J Physiol Lung Cell Mol Physiol* 2020;319:L1021–35.
48 Liang X, Xiu C, Liu M, *et al*. Platelet-neutrophil interaction aggravates vascular in fl ammation and promotes the progression of atherosclerosis by activating the Tlr4/NF-kappaB pathway. *J Cell Biochem* 2019;120:5612–9.
49 Schulz M, Dotzlaw H, Neeck G. Ankylosing Spondylitis and rheumatoid arthritis: serum levels of TNF-alpha and its soluble receptors during the course of therapy with etanercept and Infliximab. *Biomed Res Int* 2014;2014:675108.
50 Nowlan ML, Drewe E, Bulsara H, *et al*. Systemic cytokine levels and the effects of etanercept in TNF receptor-associated periodic syndrome (TRAPS) involving a C33Y Mutation in Tnfrsf1A. *Rheumatology (Oxford)* 2006;45:31–7.
51 Nishimoto N, Terao K, Mima T, *et al*. Mechanisms and pathologic significances in increase in serum Interleukin-6 (IL-6) and soluble IL-6 receptor after administration of an anti-IL-6 receptor antibody, tocilizumab, in patients with rheumatoid arthritis and castleman disease. *Blood* 2008;112:3959–64.
52 Schelbergen RF, Geven EJ, van den Bosch MHJ, *et al*. Prophylactic treatment with S100A9 inhibitor paquinimod reduces pathology in experimental collagenase-induced osteoarthritis. *Ann Rheum Dis* 2015;74:2254–8.
53 Abraham DJ, Eckes B, Rajkumar V, *et al*. New developments in fibroblast and myofibroblast biology: implications for fibrosis and scleroderma. *Curr Rheumatol Rep* 2007;9:136–43.
54 Gilbane AJ, Denton CP, Holmes AM. Scleroderma pathogenesis: a pivotal role for fibroblasts as effector cells. *Arthritis Res Ther* 2013;15:215.
55 Kendall RT, Feghali-Bostwick CA. Fibroblasts in fibrosis: novel roles and mediators. *Front Pharmacol* 2014;5:123.
56 Postlethwaite AE, Shigemitsu H, Kanangat S. Cellular origins of fibroblasts: possible implications for organ fibrosis in systemic sclerosis. *Curr Opin Rheumatol* 2004;16:733–8.
57 Lamouille S, Xu J, Derynck R. Molecular mechanisms of epithelial-mesenchymal transition. *Nat Rev Mol Cell Biol* 2014;15:178–96.
58 Huang N, Zhao G, Yang Q, *et al*. Intracellular and extracellular S100A9 trigger epithelial-mesenchymal transition and promote the invasive phenotype of pituitary adenoma through activation of Akt1. *Aging (Albany NY)* 2020;12:23114–28.
59 Kishi M, Aono Y, Sato S, *et al*. Blockade of platelet-derived growth factor receptor-beta, not receptor-alpha ameliorates bleomycin-induced pulmonary fibrosis in mice. *PLoS One* 2018;13:e0209786.
60 Harrison JH, Lazo JS. High dose continuous infusion of bleomycin in mice: a new model for drug-induced pulmonary fibrosis. *J Pharmacol Exp Ther* 1987;243:1185–94.
61 Natsuizaka M, Chiba H, Kuronuma K, *et al*. Epidemiologic survey of Japanese patients with idiopathic pulmonary fibrosis and investigation of ethnic differences. *Am J Respir Crit Care Med* 2014;190:773–9.
62 Kondoh Y, Suda T, Hongo Y, *et al*. Prevalence of idiopathic pulmonary fibrosis in Japan based on a claims database analysis. *Respir Res* 2022;23:24.
63 Fernández Pérez ER, Daniels CE, Schroeder DR, *et al*. Incidence, prevalence, and clinical course of idiopathic pulmonary fibrosis: a population-based study. *Chest* 2010;137:129–37.
64 Hopkins RB, Burke N, Fell C, *et al*. Epidemiology and survival of idiopathic pulmonary fibrosis from National data in Canada. *Eur Respir J* 2016;48:187–95.